CONF-850310--29

MASTER

CONF-850310--29

DE85 007898

MODELING OF TRITIUM TRANSPORT IN LITHIUM ALUMINATE FUSION SOLID BREEDERS*

M. C. Billone and R. G. Clemmer
Fusion Power Program, Argonne National Laboratory
9700 South Cass Avenue, Argonne, Illinois 60439
(312) 972-7146/3838

Submitted February 1985

The submitted manuscript has been authored by a contractor of the U. S. Government under contract No. W-31-109-ENG-38. Accordingly, the U. S. Government retains a nonexclusive, royalty-free license to publish or reproduce the published form of this contribution, or allow others to do so, for U. S. Government purposes.

DISCLAIMER

This report was prepared as an account of work sponsored by an agency of the United States Government. Neither the United States Government nor any agency thereof, nor any of their employees, makes any warranty, express or implied, or assumes any legal liability or responsibility for the accuracy, completeness, or usefulness of any information, apparatus, product, or process disclosed, or represents that its use would not infringe privately owned rights. Reference herein to any specific commercial product, process, or service by trade name, trademark, manufacturer, or otherwise does not necessarily constitute or imply its endorsement, recommendation, or favoring by the United States Government or any agency thereof. The views and opinions of authors expressed herein do not necessarily state or reflect those of the United States Government or any agency thereof.

DISTRIBUTION OF THIS DOCUMENT IS UNLIMITED

MODELING OF TRITIUM TRANSPORT IN LITHIUM ALUMINATE FUSION SOLID BREEDERS

M. C. BILLONE AND R. G. CLEMMER
Fusion Power Program, Argonne National Laboratory
9700 South Cass Avenue, Argonne, Illinois 60439
(312) 972-7146/3838

ABSTRACT

Lithium aluminate is a candidate tritium-breeding material for fusion reactor blankets. One of the concerns with using $LiAlO_2$ is tritium recovery from this material, particularly at low operating temperatures and high fluences. The data from various tritium release experiments with γ-$LiAlO_2$ and related materials are reviewed and analyzed to determine under what conditions bulk diffusion is the rate-limiting mechanism for tritium transport and what the effective bulk diffusion coefficient should be. Steady-state and transient models based on bulk diffusion are developed and used to interpret the data. Design calculations are then performed with the verified models to determine the steady-state inventory and time to reach equilibrium for a full-scale fusion blanket.

I. INTRODUCTION

Several fusion blanket designs have been proposed using γ-$LiAlO_2$ as the breeding material. Because of its relatively low lithium atom density (0.28 g/cm^3) and low thermal conductivity (resulting in high coolant and structure fractions in the blanket), a neutron multiplier (e.g., beryllium) and ^{6}Li enrichment are required in order to attain an acceptable tritium breeding ratio. While the problem of tritium breeding in γ-$LiAlO_2$ appears to have been solved, there is still a great deal of concern about tritium recovery from this material, particularly at low operating temperatures and high fluences.

The literature data on tritium release from γ-$LiAlO_2$ and related materials are reviewed and assessed. These data are from post-irradiation annealing experiments as well as in-reactor purge-flow and closed-capsule tests. Through modeling, an attempt is made to separate out the mechanisms of bulk diffusion, desolution, and surface desorption in order to determine the temperature dependence of the bulk diffusion coefficient and situations under which bulk diffusion is the rate-limiting mechanism. Considerable emphasis is placed on the analysis of TRIO-1 data[1,2] because of the degree of temperature and purge chemistry control in the TRIO experiment and the quality of the on-line transient release data and the steady-state retention data.

Based on the models developed and verified in this work, design calculations are made to determine the steady-state inventory as a function of minimum operating temperature for the Blanket Comparison and Selection Study (BCSS)[3] water-cooled design. The transient behavior of the blanket after an instantaneous startup is also characterized to determine the times at which the inventory and the release fractions reach 67.4% and 99% of their equilibrium values.

II. ANALYTICAL METHODS

Tritium transport in a solid-breeder blanket consists of a complex series of events. The approach adopted in this work is to develop a model based on one mechanism (i.e., bulk diffusion) and test it against the data base. The degree to which the model matches the tritium transient release data and the steady-state retention (i.e., inventory) data helps determine the temperature, microstructure, and purge chemistry conditions under which bulk diffusion is the dominant, rate-limiting mechanism. For conditions in which the predictions and the data do not agree, the difference between the model predictions and the data helps determine the magnitude of the other effects and paves the way for more sophisticated modeling.

Classical solutions exist in the heat and mass transfer literature to describe the diffusion of a gas in an isothermal, spherical grain with the grain boundary acting as a perfect sink.[4] Several of these solutions have been integrated over a cylindrical unit cell of polycrystalline material with inner radius and temperature (r_i and T_i, respectively), outer radius and temperature (r_o and T_o, respectively), and total generation rate ($\dot{G}$) to obtain analytical approximations needed for data analysis and design scoping calculations. These solutions are presented below.

A. Steady-State Inventory

The steady-state tritium inventory (I_d) due to bulk diffusion alone can be expressed as

$$I_d = f \dot{G} r_g^2/[15\ D(\bar{T})] , \quad (1)$$

where r_g is the grain radius, $D(\bar{T}) = D_o \exp(-Q/R\bar{T})$, D_o is a constant, Q is the apparent activation energy for diffusion, R is the ideal gas constant, $\bar{T}$ is the cross-sectional, area-averaged temperature, and f is a factor which accounts for the temperature variation. The factor f is given by

$$f = (\beta - 1)^{-1} \int^{\beta} \exp[(Q/R\bar{T}) \times (\bar{T}/T - 1)]\, d\eta , \quad (2)$$

where $\beta = r_o^2/r_i^2$, $\eta = r^2/r_i^2$, r is an arbitrary radius, and $T = T(\eta)$ is the local temperature.

B. Instantaneous Startup

Assuming an instantaneous increase in generation rate and temperature with zero initial tritium concentration, the transient tritium release rate ($\dot{R}$) and inventory (I) can be expressed as fractions of their steady-state values ($\dot{G}$ and I_{ss}, respectively):

$$\dot{R}/\dot{G} = 1 - (6/\pi^2) \sum_{n=1}^{\infty} (1/n^2)(\beta - 1)^{-1} \times \int^{\beta} \exp(-n^2\pi^2 t/\tau)\, d\eta , \quad (3)$$

$$I/I_{ss} = 1 - (90/\pi^4) \sum_{n=1}^{\infty} (1/n^4) \times \int^{\beta} \exp(-n^2\pi^2 t/\tau)\, d\eta \Big/ \int^{\beta} \tau\, d\eta , \quad (4)$$

where t is time, $\tau = r_g^2/D$, and I_{ss} is given by Eq. (1).

C. Instantaneous Temperature Change

For steady-state conditions at $t < 0$, a constant generation rate, and a step increase in temperature profile $[T_1(\eta) + T_2(\eta)]$, the fractional release rate and inventory can be written as:

$$\dot{R}/\dot{G} = 1 + (6/\pi^2) \sum_{n=1}^{\infty} (1/n^2)(\beta - 1)^{-1} \times \int^{\beta} (\tau_1/\tau_2 - 1) \exp(-n^2\pi^2 t/\tau_2)\, d\eta , \quad (5)$$

$$I/I_{ss2} = 1 + (90/\pi^4) \sum_{n=1}^{\infty} (1/n^4) \times \frac{\int^{\beta} (\tau_1 - \tau_2) \exp(-n^2\pi^2 t/\tau_2)\, d\eta}{\int^{\beta} \tau_2\, d\eta} , \quad (6)$$

where $\tau_1 = r_g^2/15\ D(T_1)$, $\tau_2 = r_g^2/15\ D(T_2)$, $T_1 = T_1(\eta)$, $T_2 = T_2(\eta)$ and I_{ss2} is the steady-state inventory after the temperature change.

III. ANALYSIS OF TRIO-1 DATA

The TRIO-1 in-reactor, purge-flow experiment consisted of 33 runs in which the temperature of the hollow cylindrical sample was varied from run to run along with the purge stream chemistry. Thermocouples were used to monitor the inner (T_i) and outer (T_o) surface temperatures; the generation rate ($\dot{G}$) was calculated from the neutron flux distribution which was monitored by flux detectors; and the inventory at the end of each run was calculated based on the generation rate and the tritium lost from the sample through purge stream convection and permeation. Table I summarizes the parameters for each run and the end-of-run inventory data used in this study to determine the effective bulk diffusion coefficient and the conditions under which bulk diffusion was dominant. Columns 3 and 4 give the volume-averaged temperature ($\bar{T}$) and the average radial temperature drop ($\overline{\Delta T} = \bar{T}_i - \bar{T}_o$), respectively, for each run. While the thermocouple data indicated some axial and circumferential variation in temperature, a radial heat flow model was used to estimate the temperature profile as:

$$T = \bar{T} + [0.476 - (\eta/\beta)]\overline{\Delta T} . \quad (7)$$

The parameter $(I/\dot{G})_{nom}$ was obtained by taking the ratio of the inventory and the generation rate deduced from data. The $\Delta(I/\dot{G})$ represents the one-sigma uncertainty associated with this ratio. The small uncertainty for Run 33 is due to the fact that I was determined directly from post-irradiation measurements.

An analysis of Table I indicates that Runs 1-8 and 28-33 with protium swamping show the type of temperature sensitivity one would expect from a bulk-diffusion process. Equation (1) was inverted to solve for the diffusion coefficient D as a function of the volume-averaged temperature for each of these runs. Based on pre- and post-test microstructural analysis, a grain radius of 0.1 (±30%) μm was used in the calculation. The results are shown in Fig. 1. A reasonable fit to the data was obtained by:

$$\ln(D/cm^2 \cdot s^{-1}) = (-13.7 \pm 2.3) - (35.8 \pm 3.9)\ kcal/mol/RT , \quad (8)$$

where only the one-sigma uncertainty in the ratio $(I/\dot{G})^{-1}$ was included. For purposes of comparing the results of this analysis to other experimental studies, the uncertainty in grain size is statistically included in the correlation to give:

TABLE I

TRIO-1 Test Parameters Used as Input to the Diffusivity Analysis

Run No.	Purge Chemistry	$\bar{T}$ (°C)	$\overline{\Delta T}$ (°C)	$(I/\bar{G})_{nom}$ (10^4 s)	$\Delta(I/\bar{G})^a$ (%)
1	0.1% H_2	592	126	1.70	30.4
2		677	127	1.13	91.0
3	1% H_2	685	127	1.56	88.0
4[b]	0.1% H_2	627	131	6.49	40.0
5[b]		481	131	14.0	22.6
6		530	131	8.54	39.4
7		578	130	2.73	156.0
8		627	126	0.462	1080.0
9[b]	0% H_2	630	128	15.0	42.8
10[b]		396	127	21.7	30.8
11[b]		488	128	24.5	28.0
12[b]		605	128	35.9	22.3
13		582	128	31.1	30.3
14		684	126	19.0	51.7
15	0.1% H_2	684	126	12.1	83.7
16		682	126	11.7	83.8
17		677	125	12.4	74.8
18		683	125	11.6	77.1
19		628	126	11.6	76.6
20[b]	0.2% O_2	639	116	46.0	19.0
21	0.1% H_2	639	116	40.3	21.1
22		588	117	40.9	20.2
23		533	109	48.9	16.7
24		585	109	44.7	17.7
25		546	113	47.6	16.1
26		530	109	51.9	13.2
27		513	106	46.1	11.5
28		489	107	34.5	10.1
29[b]		474	107	34.5	8.3
30		474	107	37.3	6.3
31		434	112	37.4	5.3
32[b]		531	111	20.0	5.6
33		642	113	0.498	11.4

[a]One-sigma uncertainties.

[b]Steady-state not achieved.

$$\ln(D/cm^2 \cdot s^{-1}) = (-13.7 \pm 1.8) - (35.8 \pm 3.9)\ \text{kcal/mol}/RT. \quad (9)$$

It should be emphasized that both qualitative and quantitative information is gained from this analysis. The observation that the data from Runs 1-8 and 28-33 can be rationalized by Eq. (1) is strong evidence that bulk diffusion is the dominant mechanism for tritium retention under the conditions at these runs. Namely, for fine-grain-size γ-$LiAlO_2$ samples purged by a helium stream containing excess hydrogen (0.1 vol.%), bulk diffusion dominates over other mechanisms such as surface adsorption and solubility in determining the tritium inventory in the temperature range

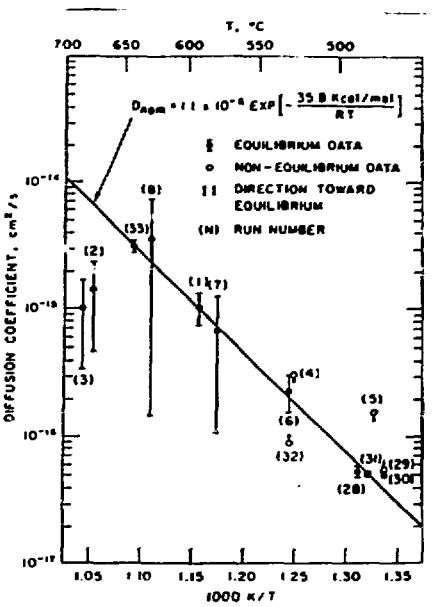

Fig. 1. Diffusion coefficient for tritium in γ-$LiAlO_2$ determined from selected TRIO runs.

of 400-700°C. Furthermore, the analysis provides a quantitative determination of the effective bulk diffusion coefficient.

An independent method was also used to assess the degree to which bulk diffusion was rate-limiting for tritium release. Several transient traces for tritium (HT) release were selected for analysis. Figure 2 shows the experimental generation rate ($\dot{G}$) and release rate ($\dot{R}_e$) for Run 8 which was subjected to an average temperature increase of 50°C. Figures 3 and 4 show the same information for Runs 28 and 31 which experienced average temperature changes of -25°C and +10°C, respectively. Included in the graphs are the analytically predicted release rates ($\dot{R}_{min}$, $\dot{R}_{nom}$, and $\dot{R}_{max}$) based on Eqs. (5) and (8). Qualitatively, the comparisons are excellent as the two temperature-increase cases (8 and 31) exhibit burst releases followed by an asymptotic approach to equilibrium which depends on the temperature of the run. The temperature-decrease case (28) exhibits the expected depression in release rate relative to equilibrium. Quantitative comparisons are difficult for two reasons. The amplitude and rate of change of the experimental release-rate curve are not as large at t = 0 as the analytical one because of the finite time (~1 hr) for the temperature rise. Also, the experimental time to reach equilibrium is hard to determine because of the ±10% uncertainty in the data. However, the trends in the data strongly suggest that bulk diffusion is rate-limiting for these runs and that Eq. (8) is a reasonable representation

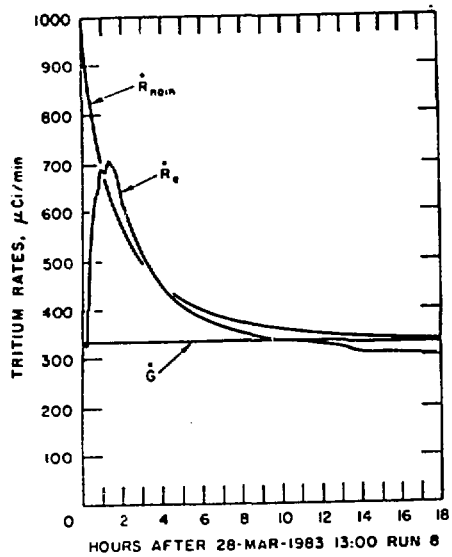

Fig. 2. Comparison of analytical predictions $(\dot{R}_{nom})$ for a step increase (50°C) in temperature at a constant generation rate $(\dot{G})$ for TRIO Run 8.

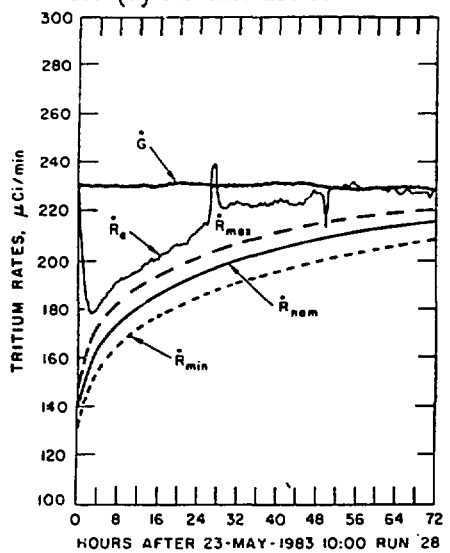

Fig. 3. Comparison of analytical predictions $(\dot{R}_{min}, \dot{R}_{nom}, \dot{R}_{max})$ and experimental results $(\dot{R}_e)$ for a step decrease (25°C) in temperature at a constant generation rate $(\dot{G})$ for TRIO Run 28.

of the diffusion coefficient for γ-$LiAlO_2$.

IV. COMPARISON WITH OTHER WORK

A number of other experiments have been reviewed and compared with the apparent diffusivities calculated from the TRIO-1 data. Elleman et al.[5,6] measured tritium diffusion in

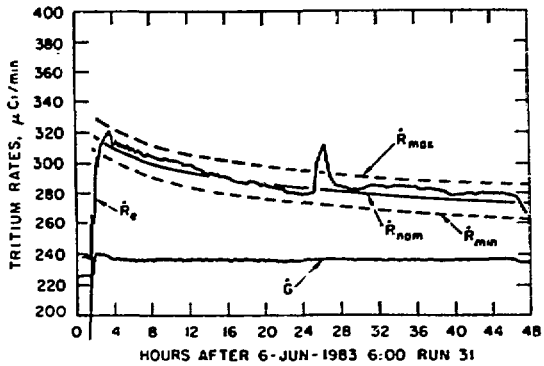

Fig. 4. Comparison of analytical predictions $(\dot{R}_{min}, \dot{R}_{nom}, \dot{R}_{max})$ and experimental results $(\dot{R}_e)$ for a step increase (10°C) in temperature at a constant generation rate $(\dot{G})$ for TRIO Run 31.

in a related material $(\alpha$-$Al_2O_3)$ by recoiling tritium into the samples and recording the transient tritium released during post-irradiation heating. The measured activation energy for the single-crystal samples was 57.1 ± 2.4 kcal/mol.

Wiswall and Wirsing[7,8] measured the response of pre-irradiated γ-$LiAlO_2$ powders and sintered pellets to post-irradiation annealing. Their results are shown in Fig. 5 for the powdered samples (70-100 mesh) at temperatures of 500, 600, and 650°C. While the grain size was not specified, a grain radius of 0.1 μm (authors report submicron fine particle sizes) was assumed.

Yunker[9] reported results for tritium diffusivity in $LiAlO_2$ in the temperature range of 400-650°C. Although no details are presented in the reference, the results are included in Fig. 5. Yunker's values of diffusivity per particle radius squared were converted to the points plotted in Fig. 5 by arbitrarily assuming a grain radius of 0.3 μm.

Botter et al[10] have performed a TRIO-type experiment (LILA) at Saclay with γ-$LiAlO_2$. Results were reported for the diffusion coefficient in ~0.2-μm-radius grains based on an analysis of transient release data in the temperature range of 430-600°C. The diffusion coefficients determined from their data are included in Fig. 5 along with the values (straight lines) determined from the TRIO-1 analysis [Eq. (9)].

V. DESIGN CALCULATIONS

Sample calculations were performed for the BCSS $LiAlO_2/H_2O$/FS/Be design to determine steady-state tritium inventory and response time. The steady-state inventory based on bulk diffusion is calculatedusing Eq. (1). The input for this study is $\dot{G}$ = 866 g/day (1.86

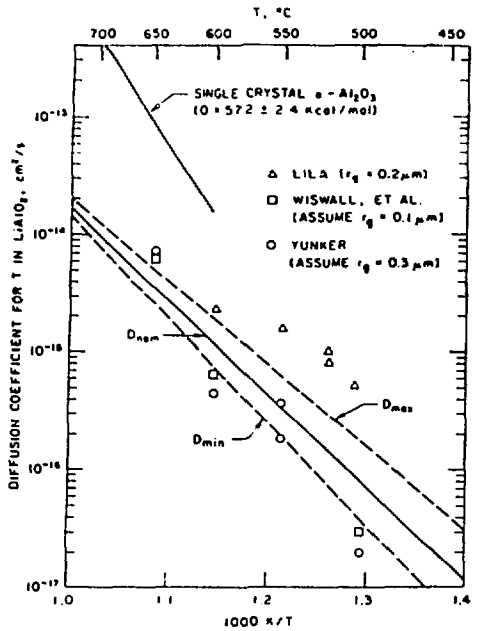

Fig. 5. Comparison of some data for tritium diffusion in γ-$LiAlO_2$ with the TRIO-1 correlation.

$\times 10^{-5}$ wppm/s), r_g = 0.1 μm, r_i = 6.5 mm, and T_{max} = 1000°C. The outer radius (r_o) of the unit cell was constrained to vary as the minimum breeder temperature (T_{min}) was varied according to the steady-state heat-transfer relationship:

$$(\beta - 1)\left[(1 - \beta^{-1})^{-1} \ln \beta - 1\right] \leq \frac{4\, k_b \Delta T}{\bar{q}_b r_i^2}, \quad (10)$$

where $\beta = r_o^2/r_i^2$, k_b = thermal conductivity (1.1 W/m·K), $\bar{q}_b$ = average heating rate (18 MW/m³), and $\Delta T = T_{max} - T_{min}$.

Figure 6 shows the predicted diffusive inventory as a function of the minimum blanket temperature (T_{min}). The sensitivity of I_d to T_{min} is clearly demonstrated in this figure. At a minimum blanket temperature of 335°C, the diffusive inventory is estimated to be ~2 to ~10 kg with a nominal value of 4.5 kg. An increase of only 15°C in T_{min} results in a 50% decrease in inventory.

Calculations have also been performed to characterize the tritium response (due to bulk diffusion) of a full-scale $LiAlO_2$ blanket to an instantaneous reactor startup. Figure 7 shows the release rate and inventory fractions for the reference $LiAlO_2/H_2O$/FS/Be blanket as a function of time. Equations (3), (4), and (9) were used for these calculations under the assumption that an average unit cell can be used to characterize the blanket response.

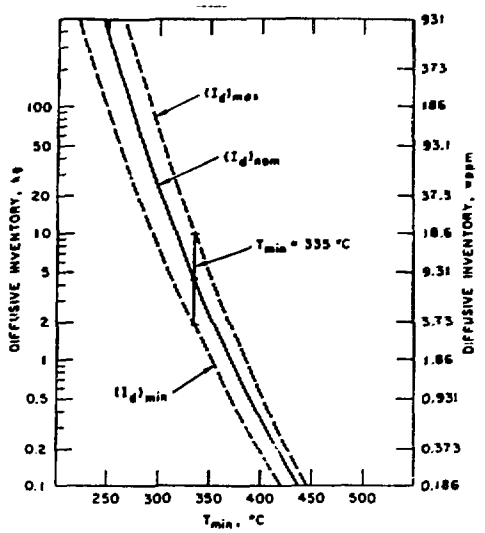

Fig. 6. Predicted inventory for the $LiAlO_2/H_2O$/HT9/Be design as a function of T_{min}.

Time is expressed in fluence units of MWy/m² (for a 5-MW/m² neutron wall loading) and in the more fundamental units of days, months, and years. The release rate reaches 67.4% of equilibrium in ~1 min and asymptotically approaches 99% of equilibrium at ~2 mo of blanket operation. The times to reach thermal equilibrium have been estimated at ~1 min for a unit cell near the first wall, ~8 min for an average unit cell, and ~45 min for a unit cell near the reflector at the back of the blanket. Therefore, the model assumption of instantaneous startup is reasonable for estimating the time to reach 99% of equilibrium tritium release rate.

The inventory is much more sluggish than the release rate. It takes ~6 mo for the inventory to build up to 67.4% of its equilib-

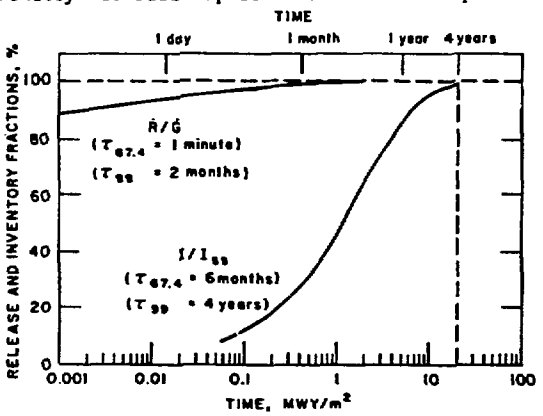

Fig. 7. Tritium response to an idealized reactor startup for the $LiAlO_2/H_2O$/HT9/Be design with T_{min} = 350°C, T_{min} = 1000°C, and r_g = 0.1 μm.

rium values and ~4 yr to reach 99% of equilibrium. The reason for this is that most of the inventory is building up in the lower temperature $LiAlO_2$ grains near the coolant tube wall. The response time for these cooler grains is quite slow.

VI. DISCUSSION

The results of the TRIO-1 experiment dramatize the impact of purge chemistry on tritium retention in fine-grained (0.1 μm radius), low density (~65% TD), γ-$LiAlO_2$ samples. The addition of ~0.1 vol.% H_2 to the helium purge gas enhances tritium release and lowers tritium inventory to the levels predicted by the bulk diffusion model. After TRIO Run 8, the hydrogen was removed (leaving H_2 impurity levels of ~3 vppm in the sweep gas) and the release rate was reduced significantly below the steady-state level causing an increase of inventory of ~1-5 wppm above the diffusive inventory. It is hypothesized that surface adsorption becomes demonant under these conditions for T > 500°C. During Run 20, oxygen (0.2 vol.%) was added to the purge gas after the hydrogen was removed. The excess inventory built up to greater than 5 wppm and was still increasing at the end of the run. It took ~30 days of swamping with protium before this excess inventory was released (in the form of HTO). Runs 28-33 with protium swamping behaved similarly to Runs 1-8, indicating no time-dependent effects during the course of the radiation.

The apparent activation energy for diffusion deduced from the TRIO-1 steady-state data and checked independently against the transient data agrees reasonably well with the results reported by Elleman et al, Wiswall and Wirsing, Yunker, and Botter et al. However, the studies of Guggi et al.[11,12] and Vasiliev et al.[13] indicate lower apparent activation energies of 13-14 kcal/mol as compared to the nominal value of 35.8 kcal/mol derived from the TRIO experiment. Sample impurities, purge gas chemistry, and the chemical effect of the breeder container may have contributed to these discrepancies.

VII. CONCLUSIONS

The effective diffusion coefficient deduced from the TRIO-1 data for tritium in γ-$LiAlO_2$ is $\ell n(D/cm^2 \cdot s^{-1}) = (-13.7 \pm 1.8) - (35.8 \pm 3.9)$ kcal/mol/RT. Bulk diffusion appears to be the rate-limiting mechanism in tritium transport and the major contributor to tritium inventory when the system is purged with helium gas containing added H_2. For a purge gas with no added H_2 and/or with added O_2, other mechanisms (e.g., surface desorption) appear to be rate limiting for T > 500°C. More research needs to be conducted in order to determine irradiation and burnup effects on tritium transport and to determine the optimum microstructure and purge chemistry for tritium transport.

ACKNOWLEDGMENT

This work was supported by the U. S. Department of Energy.

REFERENCES

1. R. G. CLEMMER et al., "The TRIO Experiment," ANL/84-55, Argonne National Laboratory (1984).

2. R. G. CLEMMER et al., "The TRIO-1 Experiment: In-Situ Tritium Recovery Results," J. Nucl. Mater. 122 & 123, 80 (1984).

3. D. L. SMITH et al., "Blanket Comparison and Selection Study," ANL/FPP/84-1, Argonne National Laboratory (1984).

4. H. S. CARSLAW and J. C. JAEGER, Conduction of Heat in Solids, Oxford University Press, New York (1948).

5. T. S. ELLEMAN, L. R. ZUMWALT and K. VERGHESE, "Hydrogen Transport in Non-metallic Solids," Proc. 3rd Top. Mtg. on Technology of Controlled Nuclear Fusion, CONF-780508, Vol. 2, 763 (1978).

6. J. D. FOWLER et al., "Tritium Diffusion in Al_2O_3 and BeO," J. Am. Ceramics Soc. 60, 155 (1977).

7. R. WISWALL and E. WIRSING, "The Removal of Tritium from Fusion Reactor Blankets," BNL-S0748, Brookhaven National Laboratory (1977).

8. R. WISWALL, E. WIRSING, and K. C. HONG, "The Removal of Bred Tritium from Solid Lithium Compounds in Fusion Reactor Systems," Proc. 14th IECEC Mtg., Boston, MA, August 5-10, 1979.

9. W. YUNKER, "Continuous Extraction of Tritium from Irradiated Lithium Aluminate," TC-1745, Hanford Engineering Development Laboratory (1980).

10. F. BOTTER et al., CEA/CEN Saclay, France, personal communication (1984).

11. D. GUGGI et al., "Tritium Release from $LiAlO_2$," Proc. Mtg. on Radiation Effects and Tritium Technology for Fusion Reactors, CONF-750989, Vol. III, 416 (1976).

12. V. G. VASILIEV et al., "Investigation of the Physical-Chemical Properties of Irradiated Inorganic Compounds of Lithium Oxides, Aluminate, and Silicates," US/USSR Workshop on Engineering and Economic Problems of ETF, Moscow and Leningrad, USSR, September 10-21, 1979.

13. G. W. HOLLENBERG, "The Effect of Irradiation on Four Solid Breeder Materials," 1st Int. Conf. on Fusion Reactor Materials, Tokyo, Japan, December 3-6, 1984.